Extended Data

Chronostratigraphic framework and age control across cores

Accurately constraining the age of Arctic Ocean sediments, particularly those corresponding to low $^{230}Th_{xs}$ and low authigenic $^{10}Be/^{9}Be$ intervals, is challenging due to the limitations of traditional dating methods. Extremely low sedimentation rates, poor carbonate preservation [1,2], and the restricted hydrographic connection of the Arctic Ocean to the global oceans severely limit the use of $\delta^{18}O$-stratigraphy and subsequent classical MIS assignment.

In their pan-Arctic synthesis, Geibert et al., 2021 identified two prominent low-$^{230}Th_{xs}$ intervals traceable across the Arctic Ocean and into the Nordic Seas. The older interval was interpreted as corresponding to MIS6 and likely predates 131 ka. A younger, less pronounced low-$^{230}Th_{xs}$ interval was attributed to MIS4 (ca. 70 – 62 ka), potentially terminating near Heinrich Event 6. A third, late-glacial minimum tentatively linked to MIS2 (~18 – 15 ka) has been reported only at high-accumulation sites near the Yermak Plateau and Fram Strait and is not clearly expressed in Nordic Seas records. As mentioned in Geibert et al. (2021), given the ongoing dispute about the age of younger Pleistocene sediments, there is not yet a strict proof that the low $^{230}Th_{xs}$ intervals occurred at the exact same time in all cores. However, for subpolar cores the age constraints are clearer.

Here, we follow most of these age assignments and further specify some of them using additional lithological observations, magnetic susceptibility (MS) correlations, extinction ages of excess ^{230}Th and ^{231}Pa, and a re-evaluation of published isotope records [4].

Fram Strait, Yermak Plateau and Barents Sea

The chronostratigraphic framework of Geibert et al. (2021) relies primarily on core PS1533-3, which contains both $^{230}Th_{xs}$ and bulk ^{10}Be concentration records [5,6]. In this core, two samples with low authigenic $^{10}Be/^{9}Be$ ratios are located slightly above two distinct dark lithological layers, the uppermost layer was taken close to a light $\delta^{18}O$ peak that marks the MIS 5/6 transition. The lower sample at 452.5 cm in late MIS6 may correspond to the dark layers in PS1235-2 and GIK23065-3.

In PS1235-2, our $^{10}Be/^{9}Be$ record is based on a limited number of measurements spanning an interglacial-glacial transition. The $^{230}Th_{xs}$ record of core PS1235-2 was correlated to GIK23059, which isotope stratigraphy is well described [7]. The lowest $^{10}Be/^{9}Be$ ratio occurs within a dark grey interval enriched in coal fragments, which likely corresponds to late MIS6 and matches a similar dark interval in GIK23065-3. These coal-rich layers have previously been interpreted as reflecting enhanced input of terrigenous organic material sourced from Siberian shelf regions [8]

Core PS2138-1 from the Barents Sea, north of Svalbard, was dated using planktic foraminiferal $\delta^{18}O$ and $\delta^{13}C$ [9,10], supplemented by AMS radiocarbon ages for the younger section. Although the $\delta^{18}O$ signal may be influenced by local meltwater effects, it broadly matches global stacks and allows assignment of marine isotope stages down to MIS6.

Lomonosov and Mendeleev Ridges

AMS radiocarbon ages from Lomonosov Ridge cores (PS2185-3/6, PS87/030-1) and PS2200-5 from the Morris Jesup Rise, combined with lithological correlations to Mendeleev Ridge records (PS51/038-4, PS72/396-5), confirm that the upper widespread low-$^{230}Th_{xs}$ interval (MIS 4) clearly predates MIS 2. Radiocarbon constraints suggest ages older than 32,500 – 34,300 ^{14}C yr for the Lomonosov Ridge [11,12] and >43,000 ^{14}C yr for the Mendeleev Ridge [13–15].

The presence of $^{230}Th_{xs}$ below both low-salinity intervals in the central Arctic and a weak $^{231}Pa_{xs}$ signal in the upper part of PS87/030-1 suggests that the lower interval is younger than ~150 ka [12]. However, significant uncertainties

remain. In some records (e.g., PS51/038-4, PS2185-3/6), *Emiliania huxleyi* has been reported below the nominal MIS 6 low-$^{230}Th_{xs}$ interval [16], implying much higher sedimentation rates. As this occurrence could not be confirmed in subsequent work (Razmjooei et al., 2023), we adopt the older age model [17] for PS2185-6, supported by recent work [4] consistent with lower sedimentation rates on the Lomonosov Ridge.

In PS2200-5, age control relies on correlation to PS2185-6 due to the scarcity of other age markers. While lithological similarities suggest a possible MIS6 assignment, the two samples with low $^{10}Be/^{9}Be$ ratios in PS2200-5 are not associated with dark or coal-bearing layers, and a late MIS6 age — analogous to southern cores — cannot be firmly inferred.

Revised interpretations for PS87/030-1 by Song et al. (2023) indicate that previously assigned MIS6 sections may be affected by a hiatus between ~62 - 65 cm depth. Combined with extinction ages of ^{230}Th and ^{231}Pa, low $^{10}Be/^{9}Be$ ratios at 23.5 and 40.5 cm are likely younger than MIS5 and may correspond to MIS4, whereas a higher ratio at 65.5 cm likely rather reflects MIS5 conditions. The presence of a *Bulimina aculeata* peak below ~70 cm, previously attributed to MIS7, further supports a stratigraphic discontinuity within the nominal MIS6 interval [12]. The hiatus during MIS6 may explain the absence of low $^{10}Be/^{9}Be$ ratio recorded around 60.5 cm depth, where Geibert et al. (2021) placed the oldest low $^{230}Th_{xs}$ event.

Nordic Seas and North Atlantic

The age model of core GIK23065-3 from the Nordic Seas is based on $\delta^{18}O$ stratigraphy [18] and MIS assignments constrained by $^{230}Th_{xs}$ [19]. In this study, GIK23065-3 is correlated using both $\delta^{18}O$ and authigenic $^{10}Be/^{9}Be$ minima during glacial intervals (Extended Data Figure 3). The late MIS6 low-$^{10}Be/^{9}Be$ interval coincides with a dark grey, coal-rich layer, consistent with enhanced terrigenous input.

The North Atlantic core MD95-2016 [20] provides independent age control, with its age model derived through alignment of planktic $\delta^{18}O$ to a probabilistic Pliocene-Pleistocene benthic $\delta^{18}O$ stack [21], following the LR04 framework [22]

Synthesis and implications

Taken together, revised extinction ages, lithological observations, and the distribution of coal-bearing layers indicate that low authigenic $^{10}Be/^{9}Be$ ratios are preferentially associated with full glacial conditions rather than intervals of elevated sedimentation rates. In some subpolar and Nordic Seas records, late MIS6 low-ratio intervals coincide with dark, coal-rich layers, consistent with enhanced supply of Siberian terrigenous material [8]. In contrast, central Arctic cores with low $^{10}Be/^{9}Be$ ratios not systematically associated with dark layers or coal enrichment, however they show an increase in smectite content, which points out to a Siberian source [23]. However, for the central Arctic cores a higher sampling resolution could help to improve stratigraphic correlation to other cores and identify late MIS6.

Accordingly, while late MIS6 represents the most consistent interval for low $^{10}Be/^{9}Be$ ratios in subpolar records, their occurrence in the central Arctic cannot be assumed to be strictly synchronous. The use of $^{10}Be/^{9}Be$ minima as stratigraphic markers should therefore be regarded as a testable working hypothesis rather than a definitive chronostratigraphic tool, particularly for central Arctic sites.

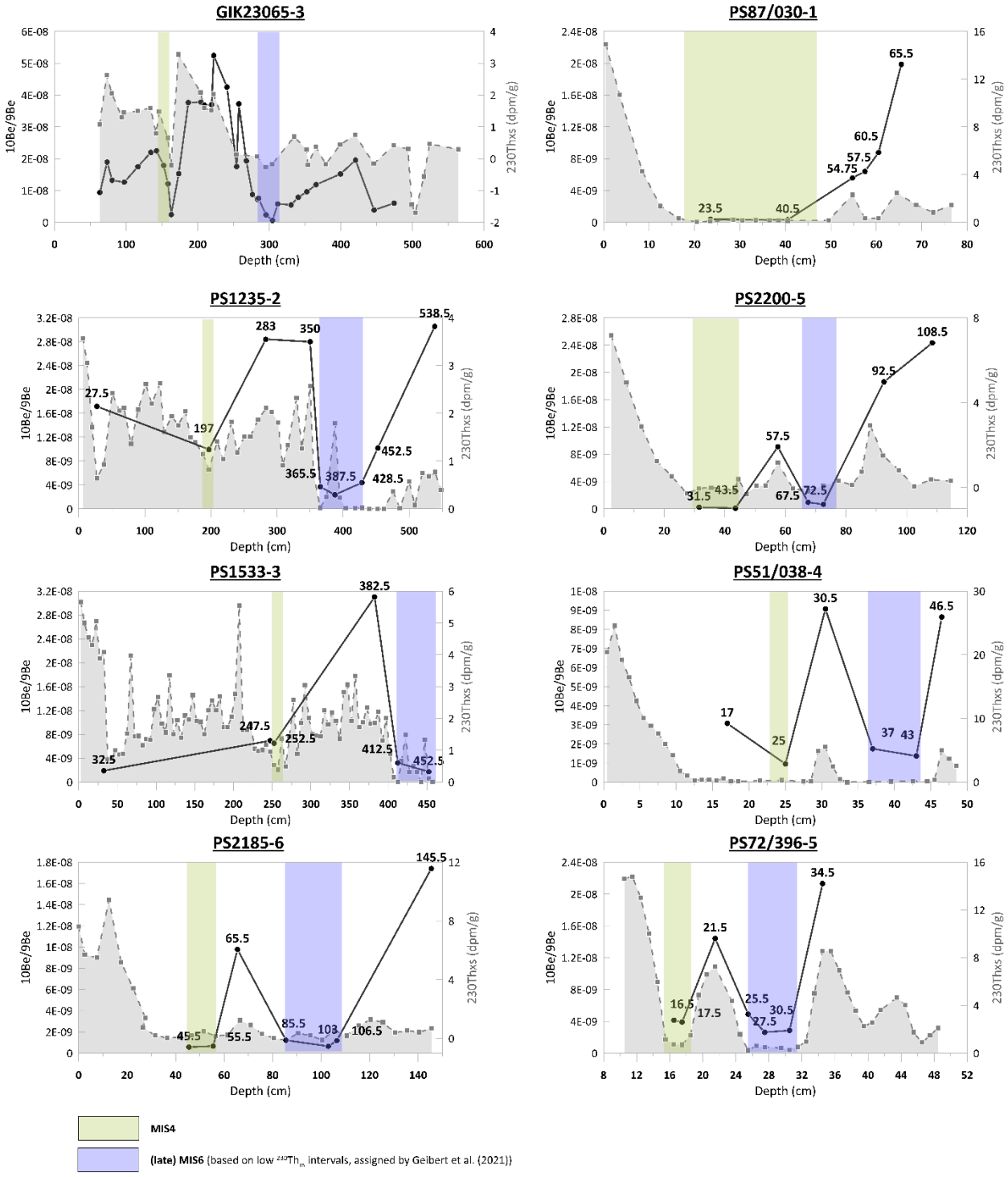

Extended Data Fig. 1 | Compilation of authigenic $^{10}Be/^{9}Be$ ratios (at/at) (in black) measured within intervals of low $^{230}Th_{xs}$ (dpm/g) reported by Geibert et al. (2021). $^{230}Th_{xs}$ records (in grey) are from Geibert et al. (2021) and references therein, except for GIK23065-3 from this study. Please note the different scales used for $^{230}Th_{xs}$. Green and blue shaded bands indicate their proposed correlations to MIS4 and (late) MIS6, respectively. Numbers denote sample depths (cm).

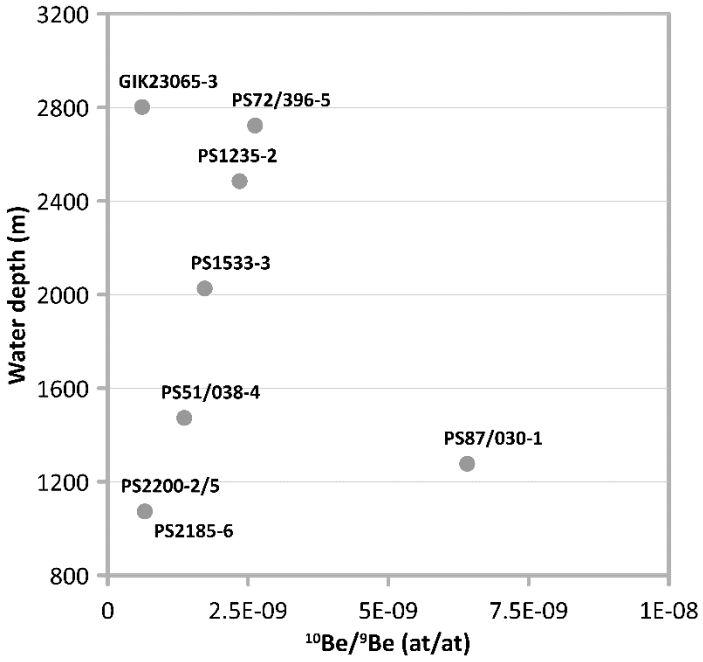

Extended Data Fig. 2 | Water depth vs. authigenic $^{10}Be/^{9}Be$ during $^{230}Th_{xs}$-minima interval (MIS6). Despite the different core locations and water depths, ranging from ~1000 m to nearly 3000 m, the $^{10}Be/^{9}Be$ ratios measured during low $^{230}Th_{xs}$ (glacial) intervals are remarkably homogeneous.

As mentioned in Main Text Fig. 1; the minima in PS87/030-1 can be explained by the presence of a hiatus of late MIS6 in the core [4]. The actual measurement could then be associated to MIS5 rather than MIS6, explaining the higher $^{10}Be/^{9}Be$ ratio.

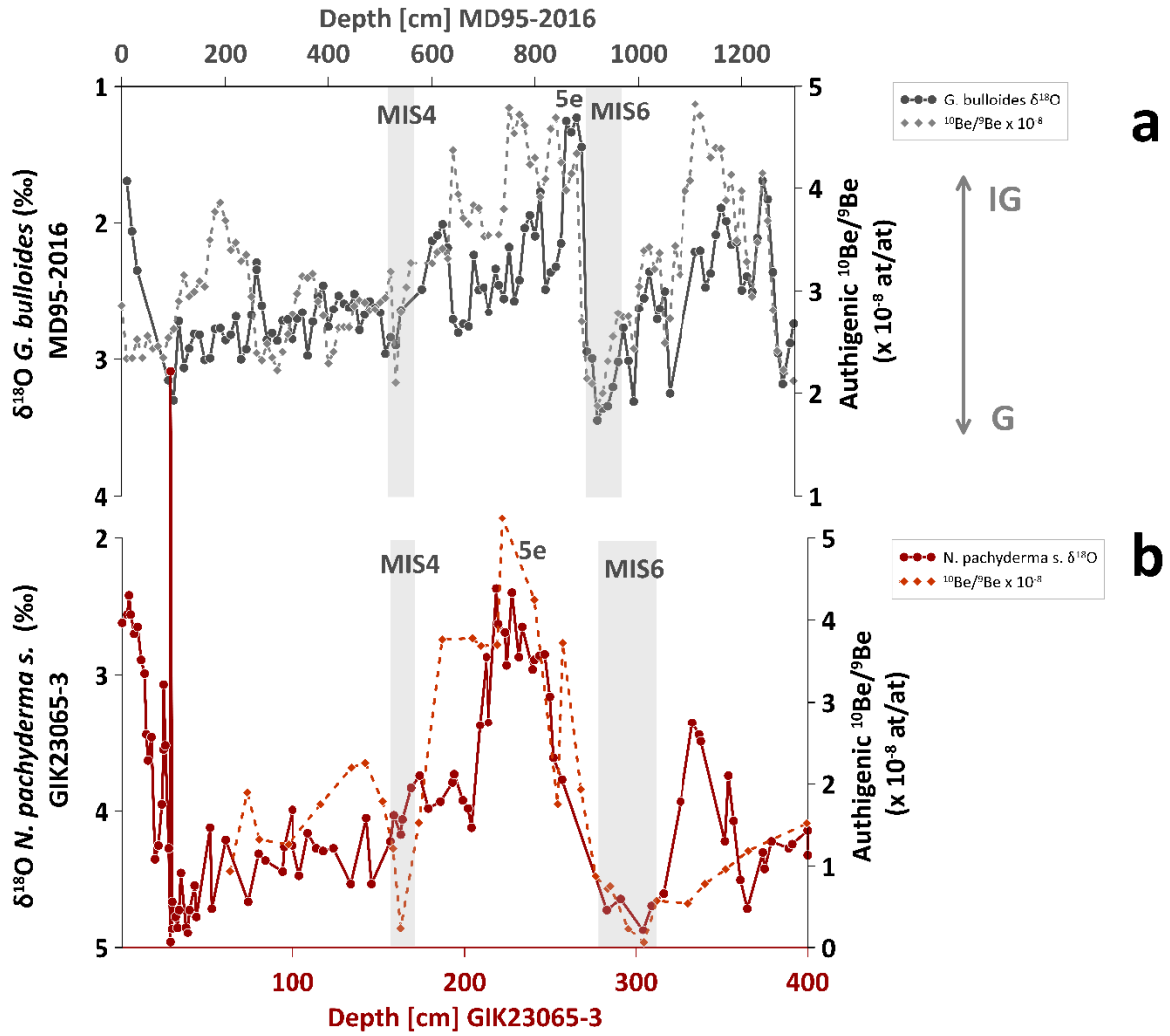

Extended Data Fig. 3 | $\delta^{18}O$ and authigenic $^{10}Be/^{9}Be$ records of MD95-2016 and GIK23065-3.
a) $\delta^{18}O$ from Savranskaia et al. (2024) has been correlated in the same study to the probabilistic benthic $\delta^{18}O$ stack from Ahn et al. (2017) (and allows a placement of MIS5 between the two grey shaded intervals marked as MIS6 and MIS4.
b) $\delta^{18}O$ and age constraints from (Vogelgesang (, 1990) used in this study for MIS6 to MIS4. The GIK23065-3 core is plotted against composite depth (and refers to GIK23065-2/3).
IG and G represent respectively interglacial and glacial periods. Authigenic $^{10}Be/^{9}Be$ ratios from MD95-2016 and GIK23065-3 are respectively from Savranskaia et al. (2024) and this study.

To anchor the low-$^{230}Th_{xs}$ intervals in a regional and global timescale, we use the MD95-2016 core's high-resolution planktic $\delta^{18}O$ record [20], which has been tied to the probabilistic benthic $\delta^{18}O$ stack (Ahn et al., 2017) and allows to constrain MIS 6 – 4 in the North Atlantic (ED Fig. 3). We then transfer this chronology to our Nordic Seas record, GIK23065-3, using the Vogelsang (1990) age model on its $\delta^{18}O$ sequence (Main Text Fig. 2b). With age control established over MIS6, 5, and 4 we compare authigenic $^{10}Be/^{9}Be$ signals in both MD95-2016 and GIK23065-3 cores (Main Text Fig. 2a and b) and extend the analysis to multiple Arctic sites (Main Text Fig. 2c).

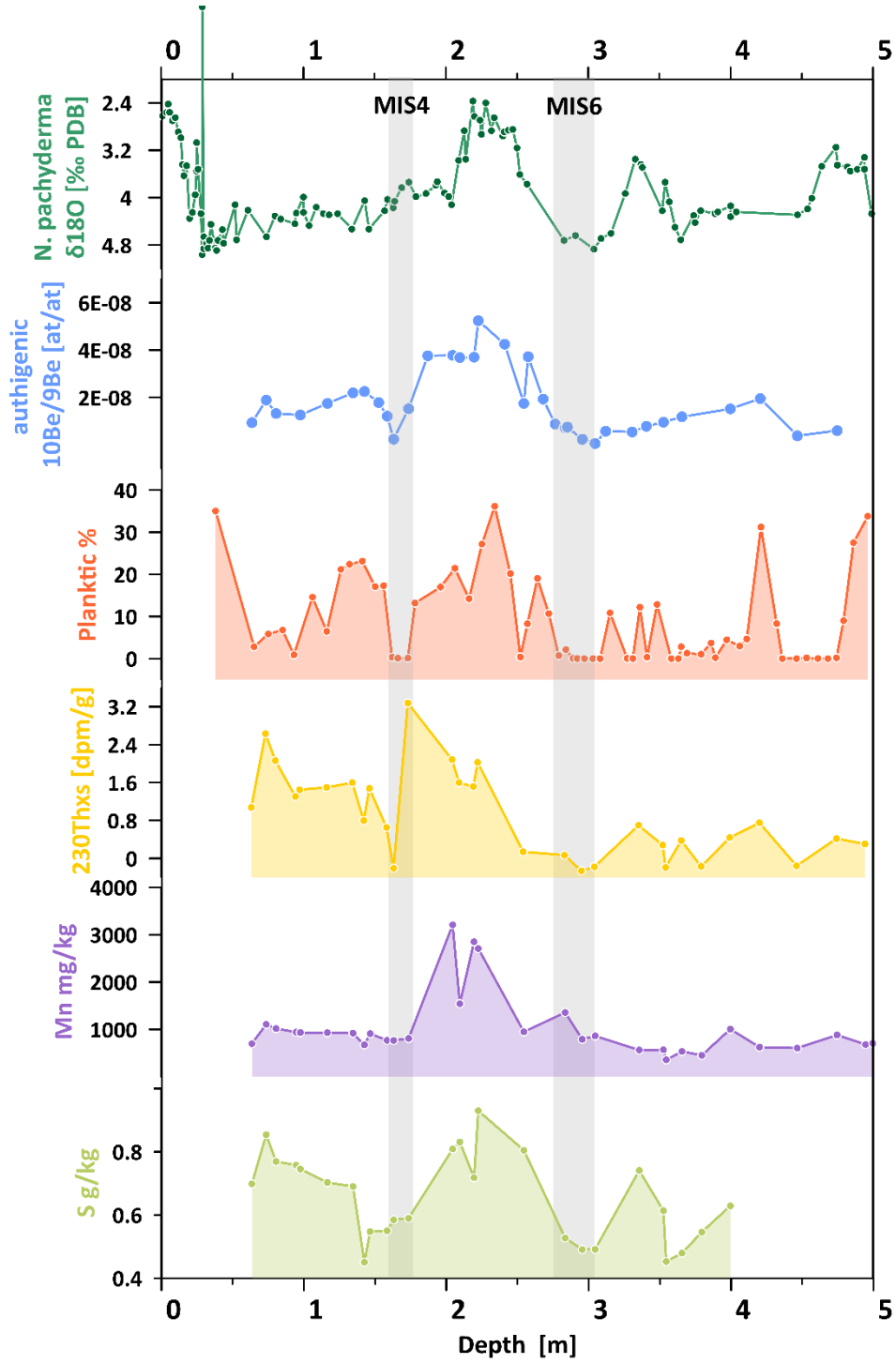

Extended Data Fig. 4 | Multi proxy analysis of GIK23065-3. N. pachyderma $\delta^{18}O$ (Vogelsang, 1990), authigenic $^{10}Be/^{9}Be$ ratio (this study), planktic foraminifera counts (percentage count of the 125 – 500 µm fraction; (Henrich, 1992), excess-^{230}Th and Mn and S (this study) are plotted together. Grey shaded bands mark glacial intervals characterized by simultaneous minima in $^{10}Be/^{9}Be$, planktic foraminifera counts, and $^{230}Th_{xs}$.

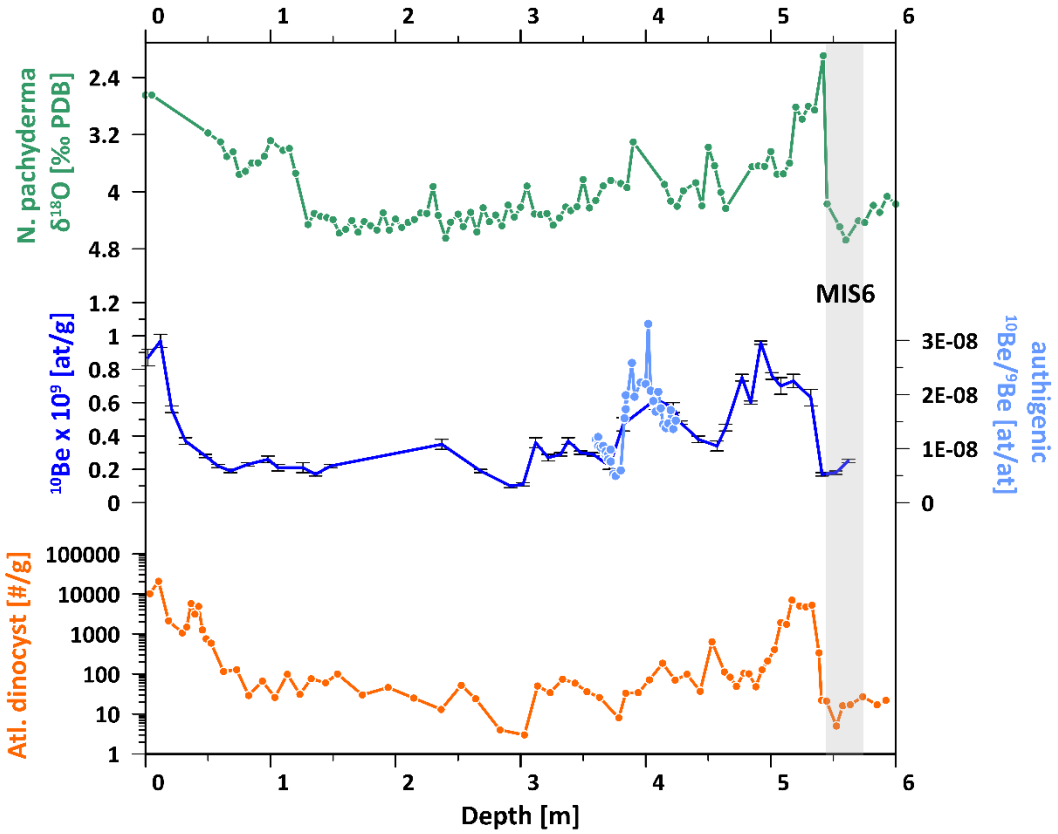

Extended Data Fig. 5| Multi proxy analysis of PS2138-1. N. pachyderma $\delta^{18}O$ and ^{10}Be-concentrations [9,25], authigenic $^{10}Be/^{9}Be$ ratio (this study), Atlantic dinocysts concentration (per unit mass,[26]) are plotted together. Grey shaded band mark glacial interval (associated to MIS6) characterized by simultaneous minima in $^{10}Be/^{9}Be$, and Atlantic dinocysts.

Sources	^{10}Be-concentrations [at/g]	^{9}Be-concentrations [pmol/kg]	Resulting ^{10}Be/^{9}Be (at/at)	Water flux
North Atlantic inflow in the Arctic Ocean	621	13.7	7.51×10^{-8}	2.1 Sv through Fram Strait 1.7 Sv through the Barents Sea
Pacific inflow at Bering Strait	200	13	2.55×10^{-8}	1 Sv through the Bering Strait
Ob	8982	1597	0.93×10^{-8}	1.28×10^{4} m^3/s
Yenisei	2935	316	1.54×10^{-8}	1.97×10^{4} m^3/s
Lena	4416	1176	0.62×10^{-8}	1.68×10^{4} m^3/s
Mackenzie	683	315	0.36×10^{-8}	9.73×10^{3} m^3/s

Extended Data Table 1 | Be isotopes concentrations from Frank et al. (2009) used as endmembers in this study's Be mass balance calculation and water fluxes.

References:

1. Backman, J., Jakobsson, M., Løvlie, R., Polyak, L. & Febo, L. A. Is the central Arctic Ocean a sediment starved basin? in *Quaternary Science Reviews* vol. 23 1435–1454 (2004).

2. Wollenburg, J. E. *et al.* Omnipresent authigenic calcite distorts Arctic radiocarbon chronology. *Commun. Earth Environ.* **4**, (2023).

3. Geibert, W., Matthiessen, J., Stimac, I., Wollenburg, J. & Stein, R. Glacial episodes of a freshwater Arctic Ocean covered by a thick ice shelf. *Nature* **590**, 97–102 (2021).

4. Song, T., Hillaire-Marcel, C., Liu, Y., Ghaleb, B. & de Vernal, A. Cycling and behavior of ^{230}Th in the Arctic Ocean: Insights from sedimentary archives. *Earth-Science Reviews* vol. 244 Preprint at https://doi.org/10.1016/j.earscirev.2023.104514 (2023).

5. Frank, M. & Eisenhauer, A. Radionuclides analysed on sediment core PS1533-3 from the Arctic Ocean. *PANGAEA https://doi. org/10.1594/PANGAEA* **50830**, (1996).

6. Eisenhauer, A. *et al.* ^{10}Be records of sediment cores from high northern latitudes: Implications for environmental and climatic changes. *Earth Planet. Sci. Lett.* **124**, 171–184 (1994).

7. Scholten, J. C. *et al. High Resolution $^{230}Th_{ex}$ Stratigraphy of Sediments from High-Latitude Areas (Norwegian Sea, Fram Strait)*. *Earth and Planetary Science Letters* vol. 101 (1990).

8. Bischof, J., Koch, J., Kubisch, M., Spielhagen, R. F. & Thiede, J. Nordic Seas surface ice drift reconstructions: evidence from ice rafted coal fragments during oxygen isotope stage 6. *Geological Society, London, Special Publications* **53**, 235–251 (1990).

9. Knies, J. *et al. Late Quaternary Growth and Decay of the Svalbard/Barents Sea Ice Sheet and Paleoceanographic Evolution in the Adjacent Arctic Ocean*. vol. 18 (1999).

10. Nowaczyk, N. R., Antonow, M., Knies, J. & Spielhagen, R. F. Further rock magnetic and chronostratigraphic results on reversal excursions during the last 50 ka as derived from northern high latitudes and discrepancies in precise AMS 14C dating. *Geophys. J. Int.* **155**, 1065–1080 (2003).

11. Nørgaard-Pedersen, N., Spielhagen, R. F., Thiede, J. & Kassens, H. Sedimentology and stable carbon and oxygen isotope record of the Central Arctic. (1998).

12. Hillaire-Marcel, C. *et al.* A New Chronology of Late Quaternary Sequences from the Central Arctic Ocean Based on "Extinction Ages" of Their Excesses in ^{231}Pa and ^{230}Th. *Geochemistry, Geophysics, Geosystems* **18**, 4573–4585 (2017).

13. Stein, R. *et al.* Towards a better (litho-) stratigraphy and reconstruction of Quaternary paleoenvironment in the Amerasian Basin (Arctic Ocean). *Polarforschung* **79**, 97–121 (2010).

14. Adler, R. E. *et al.* Sediment record from the western Arctic Ocean with an improved Late Quaternary age resolution: HOTRAX core HLY0503-8JPC, Mendeleev Ridge. *Glob. Planet. Change* **68**, 18–29 (2009).

15. Jang, K. *et al.* Glacial freshwater discharge events recorded by authigenic neodymium isotopes in sediments from the Mendeleev Ridge, western Arctic Ocean. *Earth Planet. Sci. Lett.* **369–370**, 148–157 (2013).

16. Spielhagen, R. F. *et al.* Arctic Ocean deep-sea record of northern Eurasian ice sheet history. *Quat. Sci. Rev.* **23**, 1455–1483 (2004).

17. Spielhagen, R. F. *et al.* Arctic Ocean evidence for late Quaternary initiation of northern Eurasian ice sheets. *Geology* **25**, 783–786 (1997).

18. Paetsch, H. Sedimentation im europäischen Nordmeer: radioisotopische, geochemische und tonmineralogische Untersuchungen spätquartärer Ablagerungen. (Christian-Albrechts-Universität Kiel, 1991).

19. Savranskaia, T. *et al.* Removing Climatic Overprints in Sedimentary Cosmogenic Beryllium Records: Potentials and Limits. *Geochemistry, Geophysics, Geosystems* **25**, e2024GC011761 (2024).

20. Ahn, S., Khider, D., Lisiecki, L. E. & Lawrence, C. E. A probabilistic Pliocene–Pleistocene stack of benthic δ18O using a profile hidden Markov model. *Dynamics and Statistics of the Climate System* **2**, dzx002 (2017).

21. Lisiecki, L. E. & Raymo, M. E. A Pliocene-Pleistocene stack of 57 globally distributed benthic δ18O records. *Paleoceanography* **20**, (2005).

22. Schoster, F., Behrends, M., Müller, C., Stein, R. & Wahsner, M. Modern river discharge and pathways of supplied material in the Eurasian Arctic Ocean: evidence from mineral assemblages and major and minor element distribution. *International Journal of Earth Sciences* **89**, 486–495 (2000).

23. Vogelgesang, E. *Paläo-Ozeanographie Des Europäischen Nordmeeres an Hand Stabiler Kohlenstoff- Und Sauerstoffisotope*. (Kiel, Germany, 1990). doi:10.2312/reports-sfb313.1990.23.

24. Henrich, R. Beckenanalyse des Europäischen Nordmeeres: pelagische und glaziomarine Sedimentflüsse im Zeitraum 2.6 Ma bis rezent. *Math.-Nat. Fak., Univ. Kiel. Unpubl. Habil -thesis* (1992).

25. Knies, J. & Stein, R. New aspects of organic carbon deposition and its paleoceanographic implications along the northern Barents Sea margin during the last 30,000 years. *Paleoceanography* **13**, 384–394 (1998).

26. Matthiessen, J., Knies, J., Nowaczyk, N. R. & Stein, R. *Late Quaternary Dinoflagellate Cyst Stratigraphy at the Eurasian Continental Margin, Arctic Ocean: Indications for Atlantic Water Inflow in the Past 150,000 Years*. *Global and Planetary Change* vol. 31 www.elsevier.comrlocatergloplacha (2001).